MULTILEVEL APPROACHES TOWARD MONITORING AND CONTROL OF SEMICONDUCTOR EPITAXY

D. E. ASPNES*#†, N. DIETZ,*# U. ROSSOW,*§ and K. J. BACHMANN#
*Department of Physics, North Carolina State University, Raleigh, NC 27695-8202
#Department of Materials Science and Engineering, North Carolina State University, Raleigh, NC 27695-7907
†Corresponding author: aspnes@unity.ncsu.edu
§Now at Institute of Physics, Ilmenau, Germany

ABSTRACT

Various optical techniques have been developed over the last few years to allow real-time analysis of regions of importance for semiconductor epitaxy, in particular the unreacted and reacted parts of the surface reaction layer (SRL) and the near-surface region of the sample. When coupled with emerging microscopic methods of calculating optical properties, these approaches will allow several levels of control beyond that which has been currently demonstrated.

INTRODUCTION

Electronics and optoelectronics technologies are based on artificial materials and structures, which are becoming increasingly complex as new levels of performance are achieved [1,2]. This trend will clearly continue, with devices becoming smaller and more complex, tolerances becoming more stringent, and materials being tailored according to function rather than compatibility with a particular growth process. Present requirements also include lateral patterning, selective-area deposition, and scale-up to industrial production levels. This has generated a second trend away from physical deposition techniques such as molecular beam epitaxy (MBE) toward chemical-beam methods such as organometallic chemical vapor deposition (OMCVD) and chemical beam epitaxy (CBE), where the extra dimension of chemistry can be used for greater capabilities and flexibility [3,4]. At the same time, yields must be maintained at acceptably high levels.

These trends have created a strong incentive to develop a better understanding of growth processes and better methods of monitoring growth, ideally leading to sample-driven closed-loop feedback control of the growth process itself. Much present effort is being directed toward accurately measuring process parameters and accurately modeling growth, mainly because numerous probes are available to provide a relatively detailed assessment of the ambient. However, this strategy is clearly limited in its capability to deal with complex nonlinear processes, as for example OMCVD where the surface plays an integral role in decomposing precursor species and small changes of ambient compositions can affect growth substantially [3,5].

The device that best represents current challenges is the vertical-cavity surface-emitting laser (VCSEL) [6]. VCSELs may contain hundreds of layers of varying compositions and thicknesses, which are grouped into the distributed Bragg reflectors (DBRs) at the top and bottom and an active region in the middle. At deposition rates of 1 μm/h about 6 h are required to grow a VCSEL device structure. The probability that deposition rates determined at the beginning of growth will be the same at those at the end is relatively small, especially for MBE. For this reason considerable effort has been invested in adapting and extending reflectance monitoring techniques [7] that were developed over the last 20 years by the optical thin films industry to

Mat. Res. Soc. Symp. Proc. Vol. 448 © 1997 Materials Research Society

the growth of VCSEL substructures, specifically DBRs [8-10]. However, while reflectometry can deal adequately with layers that are thick enough to generate interference patterns, it cannot cope with the 20 Å thick quantum wells that comprise the active region of the VCSEL, or for that matter the thin layers characteristic of communications lasers in general. Here, thicknesses must be maintained to within a monolayer (ML) and compositions of $In_xGa_{1-x}As_{1-y}P_y$ maintained to within several percent, or the wavelength will be outside allowable tolerances [2]. These capabilities are completely beyond reflectometric techniques, and phase-sensitive approaches such as spectroellipsometry (SE) must be used.

Growth is a surface process, so it might appear that the numerous surface-diagnostic techniques that have been developed over the years could be used to advantage in semiconductor epitaxy. However, $In_xGa_{1-x}As_{1-y}P_y$ growth necessarily involves As and P, volatile constituents that are incompatible with surface-analytic equipment. In addition growth is often done in near-atmospheric pressure environments where standard surface diagnostics cannot be used. The only generally usable conventional technique is quadrupole mass spectrometry (QMS), which with suitable differential pumping can be used in high pressure environments. However, QMS measures only reaction byproducts and hence does not address growth surfaces directly. Reflection high energy electron diffraction (RHEED) can be used in ultrahigh vacuum (UHV), but RHEED provides information only about long-range order, which is of limited utility in establishing details of the growth chemistry. Until the recent development of the surface-optical approaches discussed below [11-13] and the recent application of grazing-incidence X-ray scattering (GIXS) [14,15] to OMCVD growth, OMCVD could only be investigated by gas-phase analysis of downstream reaction products.

This lack of suitable diagnostic tools has stimulated much of the activity behind the development of optical probes over the last 10 years as discussed in recent reviews [16-19]. Optical probes are nondestructive, noninvasive, and can be used in any transparent ambient. In addition, their diagnostic capabilities have been well developed in applications to thin films [7,20] However, optical measurements have not contributed significantly to surface analysis because photons interact only weakly with materials, and the interpretation of optical data is not straightforward. The sensitivity issue can be appreciated by noting that penetration depths of light are rarely less than 100 Å, whereas the surface is about 1 Å thick. Thus the information content in a reflected beam will be divided roughly as 99% bulk and 1% surface. However, various optical techniques have recently been invented or refined to improve our capabilities for isolating the 1% surface contribution. Relatively recently developed techniques include reflectance-difference (-anisotropy) spectroscopy (RDS/RAS) [11-13,21,22], surface photoabsorption (SPA) [23,24], and p-polarized reflectance spectroscopy (PRS) [25-27]. Techniques currently undergoing rapid refinement are second-harmonic generation (SHG) [18,28] and light/laser light scattering (LS/LLS) [29-31]. As will be discussed below, all rely on symmetry in one form or another to suppress the bulk response in favor of the surface component.

The interpretational issue consists of two parts. First, the spectral range of quartz-optics systems, about 1.5 to 6.0 eV, is severely limited relative to that attainable with electron spectroscopies. This translates into a lack of specificity regarding both materials and processes. Second, without a suitable atlas of spectra of surface species it has been necessary to rely on theoretical calculations to interpret structure in surface-optical spectra. This is an extremely difficult task. Recent experiments have demonstrated that many-body effects such as localization and propagation of the excited electron are involved as well as similar effects such as screening [32]. However, new approaches where the system is treated as a coherent superposition of scattering centers offer some prospect that this problem will be solved [33,34].

The emphasis on the use of surface-analysis techniques with semiconductor epitaxy stems not so much from practical considerations as from historical reasons, specifically from the fact that RHEED has been and still remains the primary diagnostic tool for MBE. Unfortunately, this emphasis misses an essential point. Growth chemistry is established in large measure by the choice of growth technique, so the main practical considerations deal with layer thicknesses and compositions. These *bulk* properties are more efficiently and accurately determined by bulk probes such as reflectometry and ellipsometry. Although reflectometry and ellipsometry have been used for over 100 years to determine average thicknesses and compositions of deposited films [35], in compositional control the interest lies in determining *fluctuations* from a target value, ideally over a region whose thickness is vanishingly small. This *near-surface* region has recently become accessible through the development of the virtual-interface (V-I) approach, where the near-surface composition is extracted by a suitable analysis of kinetic ellipsometric data. This has led to the first (and so far only) demonstration of sample-driven closed-loop feedback control of epitaxy [36].

GROWTH: WHAT WE KNOW, WHAT WE WOULD LIKE TO KNOW

For discussion purposes we can consider the main regions relevant for epitaxial growth to be the ambient, the surface reaction layer (SRL), and the sample, as shown in Fig. 1. The SRL can be subdivided into two parts: the (mainly) physisorbed species that are weakly bound to the substrate and not in registry with it, and the (mainly) chemisorbed species that are strongly bound to the substrate and acquire the symmetry of its outermost atomic layer. This distinction is important because different optical techniques have different sensitivities to these two regions. The sample can also be subdivided into two regions: a near-surface part that contains the most recently deposited material, and the underlying bulk material. This distinction is made because we must distinguish compositional fluctuations, which must be detected and corrected with as little delay as possible, from the average composition of the film. In practice the thickness of the near-surface region is determined by the signal-to-noise capabilities of the instrumentation. For thickness control the important quantity is the bulk.

The various regions are related as follows. The ambient is established by the process parameters and consists of the carrier gas (if any) and the nutrient species providing the constituent elements to the growth surface. Some growth chemistry, such as thermal cracking of precursor species, may occur in the ambient. The nature and composition of the weakly and strongly bound parts of the SRL depend on competition between that region and the two adjacent regions and on the reactions taking place within the regions. Thus the nature and composition of the weakly bound part of the SRL depend on its reactions with the ambient and the strongly bound part, while that of the strongly bound part depends on its reactions with the weakly bound part and the near-surface region of the sample.

It is also useful to summarize the information needed to describe growth. One possible list of parameters is provided in Table I. We identify 3 categories: primary, secondary, and tertiary. The primary category contains only bulk parameters: layer thicknesses, compositions, and uniformities, because if it is not possible to meet specifications at this level the remaining parameters do not matter. The secondary category contains parameters that are surface-determined: efficiency of dopant incorporation, possibility of atomic ordering of nominally random alloys, interface widths, etc. Tertiary parameters are those related to the process itself, including for example type, pressure, and flow rate of the carrier gas, the partial pressures of active species, sample temperature, etc.

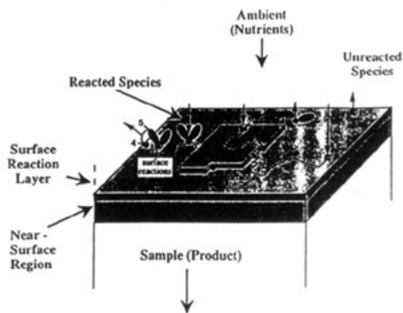

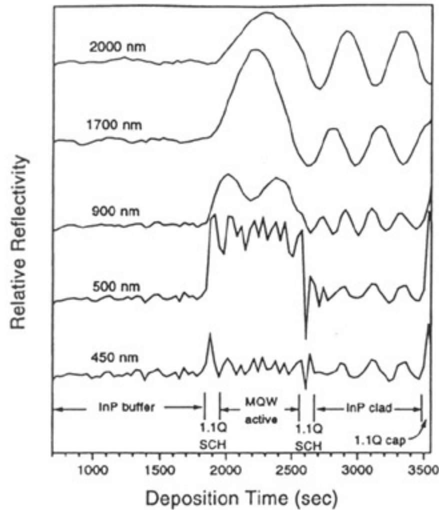

Fig. 1. Schematic diagram of the various regions of importance to epitaxial growth.

Fig. 2. Reflectance spectra obtained during the growth of a 1.3 μm InGaAsP multiquantum well laser device structure (after ref. 10).

Table I. Parameters involved in crystal growth.

Parameter:	Category:	Technique:
Primary:		
Thickness	Bulk	SR, SE
Composition	Near-surface	KE
Uniformity	Proximal	Imaging techniques
Secondary:		
Dopant incorp.	Surface-	RHEED,
Atomic ordering	determined	LS/LLS, RDS,
Interface widths		SPA, PRS, SHG
Tertiary:		
Sample temp.	Process-	TC, pyrometry
Ambient pressure,	related	ultrasonics, LIF,
temperature, species,		IRAS, CARS,
fluence...		UVAS, QMS, etc.

The tertiary parameters have received the most attention because of the expectation that sufficiently accurate measurements of process parameters together with sufficiently accurate modeling of the growth process will allow samples to be grown to the necessary degree of accuracy. However, there are several problems with this approach. First, the weakest link to the product is that formed by the ambient. Second, growth is inherently a nonlinear process and therefore difficult to model to needed levels of accuracy, especially for chemical beam methods

where the surface plays an important part in the decomposition of precursor species [3,4]. Third, small changes in ambient conditions, for instance the addition of a dopant species, can modify active surface sites and thus change growth chemistry significantly [4]. Fourth, process parameters must be measured to unrealistically high accuracies, as evidenced by the fact that most growth stations are brought on line by producing test samples and modifying conditions empirically. Finally, every growth station is distinct with its own peculiar characteristics, which makes model portability problematic.

Given the above, it would appear that a far better strategy would be to determine as much as possible about the intervening stages and to use all available information, ambient through near-surface region, as input to the control process. This is the objective of our current program. By accessing the different regions directly it is not only possible to gain a better understanding of the growth process but also to detect and correct difficulties as they occur. Also, much of the complexity of modeling is bypassed, and the burden on process parameters is reduced to that of ensuring a reasonably stable growth environment. The near-surface region needs to be considered specifically because it provides the first opportunity to determine what is actually being produced.

The ability to do this is predicated on our ability to obtain information about these regions. Most of the listed optical techniques are discussed in connection with Table II and some examples of their use are given in a following section. The process-directed probes include thermocouple measurements (TC), laser induced fluorescence (LIF), infrared absorption spectroscopy (IRAS), coherent anti-Stokes Raman scattering (CARS), and ultraviolet absorption spectroscopy (UVAS).

OPTICAL APPROACHES

At present a number of optical probes are available for addressing the bulk, near-surface, and surface regions of Fig. 1, as summarized in Table II. Bulk probes include spectroreflectometry (SR), spectroellipsometry (SE), and photoreflectance (PR). At present photoreflectance is used mainly in off-line analysis of compositions, dopant levels, damage, etc. [37,38]. Near-surface analysis can be performed by kinetic ellipsometry (KE) in connection with virtual-interface (V-I) theory [39].

Regarding surface analysis, we distinguish between *surface-oriented* and *surface-specific* approaches. The former are sensitive to surface effects but cannot return unambiguous information with samples under steady-state conditions. Although SR and SE are bulk probes, surface conditions affect these data at the nuisance (few-percent) level, i.e., enough to affect accuracy adversely but not enough to be useful for surface analysis. The surface-specific techniques can return information about surfaces under steady-state conditions. Of these, IRAS is useful mainly at wavelengths where the sample is transparent. Grazing-incidence X-ray spectroscopy returns information about long-range order but at present it can only be performed with synchrotron sources.

Of the surface-specific approaches, LS/LLS is the simplest to implement since it can be done by monitoring nonspecularly scattered light from a high intensity source such as a laser. LS/LLS provides useful information ranging from growth kinetics through relaxation of defects. SHG isolate the contribution of the lower-symmetry surface by capitalizing on polarization selection rules that are more detailed than those used in linear optics [18,28]. However, SHG equipment is too bulky to be compatible with the space limitations near growth chambers. As compact, high-power, short-pulse solid-state lasers become available SHG will become an important

Table II. Optical probes for surfaces and interfaces.

Bulk-oriented:	
SR	Spectroreflectometry
SE	Spectroellipsometry
PR	Photoreflectance
Near-surface oriented:	
KE	Kinetic ellipsometry with V-I theory
Surface-oriented:	
SDR	Surface differential reflectance
SPA	Surface photoabsorption
PRS	p-polarized reflectance spectroscopy
SR	(in kinetic mode)
SE	(in kinetic mode)
Surface-specific:	
RDS/RAS	Reflectance-difference/anisotropy spectroscopy
SHG	Second-harmonic generation
LS/LLS	Light/laser light scattering
IRAS	Infrared absorption spectroscopy
GIXS	Grazing-incidence X-ray scattering

diagnostic tool for surfaces and interfaces. The present situation has been well summarized by McGilp [18].

SPA and PRS are both variations of the original surface differential reflection (SDR) spectroscopy work of the Rome group in the late 1970s [40]. SDR is done at normal incidence, while SPA and PRS are performed with p-polarized light at the pseudo-Brewster or Brewster angles, respectively. Suppression of the bulk reflectance enhances the relative surface contribution, and also the signal-to-noise ratio relative to SDR. For PRS, which is applied in the transparent or weak absorbent wavelength range, the surface related contribution is superimposed on interference fringes which allow one to obtain additional information about the deposition rate. However, since SDR and SPA data are obtained by modifying the state of the surface, it is not always possible to establish with certainty which (if either) surface termination gave rise to the observed surface component of the signal.

RDS/RAS avoids this "which-surface" ambiguity by taking advantage of the lower symmetry of the surface relative to the bulk of cubic semiconductors. Here, the optical anisotropy of the sample is determined at normal or near-normal incidence. Since cubic materials are optically isotropic, the main contribution to RD spectra is due to the surface. Since SPA, PRS, and RDS/RAS all involve surfaces it should not be surprising that these data are all connected, as has been shown both analytically and experimentally [41,42].

EXAMPLES

We illustrate the performance capabilities of some of the above approaches by several examples. Lum et al. recently extended a multiwavelength SR configuration introduced by Killeen and co-workers [8,9] to monitor the growth of a 1.3 μm InGaAsP laser device structure [10]. The reflectometer features optical fibers to transmit and collect the reflected light and a Si/PbS

dual detector with a combined wavelength range of 400 to 2500 nm. Data of at several wavelengths are given in Fig. 2. The device structure consisted of an InP substrate, a 1.1 μm composition InGaAsP confinement layer, the multiquantum well stack with a repeat period of 17 nm, a top 1.1 μm confinement layer, an InP cladding layer, and a 1.1 μm cap. The data obtained at 450 and 500 nm wavelengths permit the individual MQW structures to be resolved, while those at longer wavelengths allow the thicknesses of the various regions to be determined. Interference oscillations in the envelope also provide information about layer thicknesses.

In Fig. 3 we show KE data obtained during sample-driven closed-loop feedback control of the growth of a 200 Å wide $Al_xGa_{1-x}As$ parabolic quantum well [36]. The structure was grown by beam epitaxy with triisobutyl (TIBAl), trimethylgallium (TMG), and cracked arsine (AsH_3) sources. The solid line in the top part of the figure shows the target composition as a function of position in the structure. The points represent the composition determined from the ellipsometrically measured pseudodielectric function $<\varepsilon>$, where the time dependence of $<\varepsilon>$ was analyzed by V-I theory for the dielectric function of the outermost region, which in turn was related to the composition x by a previously determined empirical expression. The middle is the difference between target and experimental values, and shows that composition was held to target values to within about 3%. The bottom shows the control voltage fed to the TIBAl mass flow controller while the experiment was in progress, the flow rate of which was used to establish the composition. The control voltage exhibits a noticeable asymmetry, probably due to the gettering of TIBAl as the flow increased. These results were obtained with a deposition rate was 0.95 Å/s, a sampling (including analysis) interval of 650 ms, and 5 points of averaging, meaning that the observed precision was obtained by the analysis of about 3.1 Å of material, approximately 1 ML.

The third example deals with the use of RDS to determine ML thicknesses during the OMCVD growth of a 30-period InGaAs/GaAs superlattice consisting of 5 and 10 ML thick InGaAS and GaAs layers, respectively [43]. Figure 4 shows the complete RD data set obtained at 2.6 eV, which corresponds to the peak of the As dimer structure of the (001) GaAs surface. The envelope exhibits interference oscillations, which allows the overall thickness to be determined. The 26th period is expanded at the bottom, and shows the RD oscillations with a thickness period of 1 ML.

The fourth example deals with temperature effects. Figure 5 shows SPA data obtained during exposure of an AsH_3-saturated (001) GaAs surface to trimethylgallium (TMG) at various substrate temperatures [24]. The objective is to determine conditions of atomic layer epitaxy (ALE), where growth becomes self-limiting at 1 ML such that extremely uniform layers can be deposited. Figure 5 shows that at 450 °C the growth rate decreases at 1 ML but does not stop. However, at 470 °C an ALE region is clearly defined. At 490 °C growth once again proceeds without interruption at the ML level. These data give direct information about *surface* temperatures that would be very difficult to obtain in any other way.

Finally, Fig. 6 illustrates diagnostic possibilities with the simultaneous use of various probes. Here, data are obtained for pulsed exposure to reactants during interruption of otherwise continuous heteroepitaxial growth of GaP at 350 °C [27]. The pulse sequence of tertiarybutylphosphine (TBP) and triethylgallium (TEG) is shown at the bottom. The PR and LLS data were obtained at 632.8 nm using the same HeNe laser source. The RD data were obtained at 2.6 eV. The relatively constant LLS signal indicates no substantial changes of surface morphology, such as the accumulation of Ga droplets, with the various exposures. Both the PR and RD signals show considerable changes that are not time-correlated with each other, and which continue to evolve even after exposure to the reactant has been terminated.

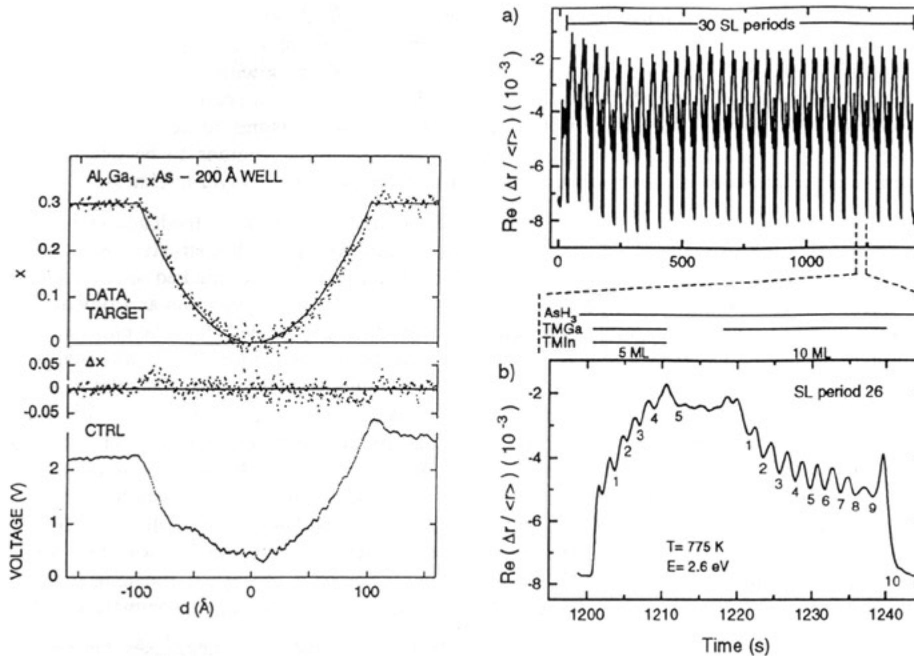

Fig. 3. Compositional data for a 200 Å wide parabolic quantum well grown by sample-driven closed-loop feedback control of epitaxy. Top: data and target values; middle: difference; bottom: control voltage. Growth and measurement parameters are given in the text (after ref. 36).

Fig. 4. Top: RD response measured during the growth of a 30-period InGaAs/GaAs superlattice consisting of 5 and 10 ML of InGaAs and GaAs, respectively. Bottom: expanded scale showing the RD oscillations allowing growth to be followed on a ML scale (after ref. 43).

The RD response, which follows primarily surface reconstruction, is much faster than the PR response, which is sensitive to composition as well, especially for TEG exposure. This shows that the reconstruction is established first, followed by a conversion of the reactant species to an intermediate which then decomposes further to donate a Ga atom to the growing crystal. When the surface is exposed to TBP the RD signal shows that the original reconstruction is obtained almost immediately. The slower PR response does not return to its original level, indicating deposition of GaP. For the double TEG sequence the PR signal is essentially repeated in both halves, while the RD signal shows an additional change indicating that further TEG exposure generates another reconstruction. The behavior of the PR signal with pulsed exposure shows directly that it contains information about both the dielectric response of the SRL and about the amount of material deposited.

A complete analysis of these data would require (1) a spectral capability and either (2) an atlas of spectra of the different species or (3) an accurate theoretical calculation of such spectra. As mentioned above, the latter is presently a difficult challenge, but one that needs to be solved if the full diagnostic power of surface-optical spectroscopy is to be realized.

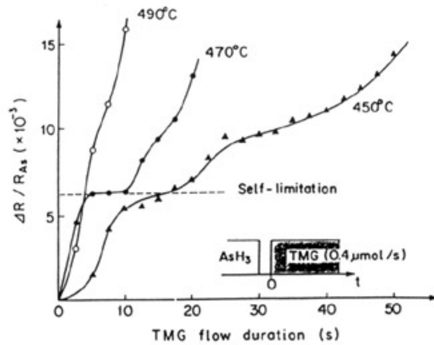

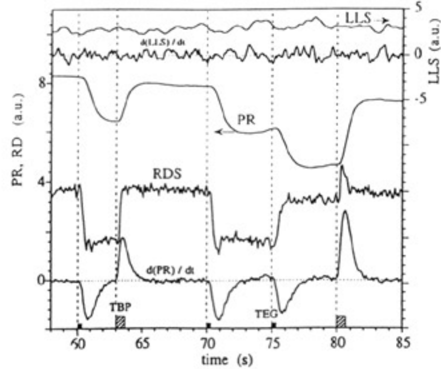

Fig. 5. Determination of a temperature range where atomic layer epitaxy occurs in the AsH_3-stabilized (001) GaAs — trimethylgallium system (after ref. 24).

Fig. 6. PR, RD, and LLS responses for single TEG and TBP pulses of 0.5 s duration during interruption of otherwise steady-state growth of GaP at 350 °C (after ref. 27).

A GENERAL CONTROL APPROACH

In general, control has meant post-mortem analysis of sample properties followed by correction of process parameters such that succeeding runs better meet specifications. While this is a reasonable first-line approach, it cannot be applied to compositionally graded structures nor can it achieve results comparable to real-time measurements and analysis, where errors can be corrected during growth. Although sample-driven closed-loop feedback control has been realized in simple situations involving ternary materials [36], improvements are needed especially for more complex systems. Ideally control decisions should be based on information obtained as close as possible to the elementary growth step where the constituent atoms are actually incorporated into the crystal lattice, typically at kinks in surface steps. This requires information about the chemical kinetics of the SRL, which is the intermediary between the process and the product, yet which to date has not been considered explicitly in the control process.

Based on the above it is clear that control of semiconductor epitaxy must evolve into a multifaceted process where information about each region is provided by specific probes and reduced by model calculations to required parameters. A general schematic is given in Fig. 7, with time increasing along the *region* axis from left to right and the *information* axis from top to bottom. The schematic diagram includes two analytic modules: scattering theory and surface chemistry; a control module; and a process module. The scattering theory and surface chemistry modules deal with the interpretation of the optical data and modeling the growth process, respectively. The surface-chemistry module includes and extends the conventional approach where growth is modeled on the basis of process information alone. The scattering-theory module deals with the analysis of the optical data. The scattering-theory model uses a database of the wavelength-dependent polarizabilities of the different species that in principle make up the unreacted and reacted parts of the SRL, allowing these concentrations to be determined. This model in principle involves calculations at the level of individual polarizable species, and can therefore accommodate local-field effects, chemical complexes, and nonspecular scattering

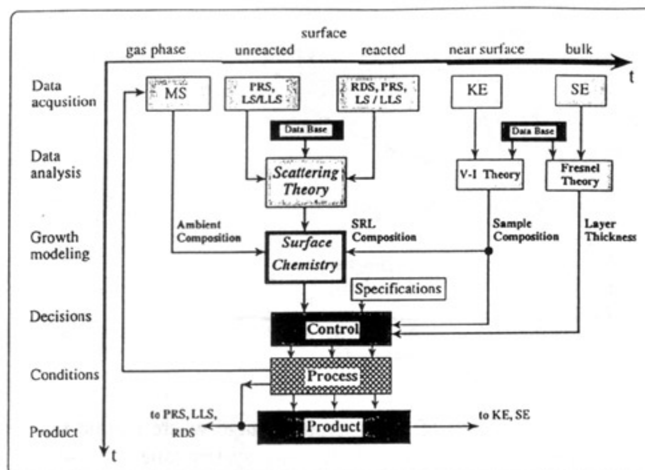

Fig. 7. General control system schematic, as discussed in the text.

by rough surfaces.

In Fig. 7 the information delivered by the probes are fed to the appropriate modules, analyzed, and sent to the control module, which compares this information to target values and adjusts process parameters accordingly. Here, we assume that information about the ambient is obtained by QMS, that concerning the unreacted part of the SRL by PRS, and that of the reacted part by a combination of RDS, PRS, and LLS. Near-surface information is obtained by KE in connection with V-I theory. Although this system remains to be implemented, the component capabilities have already been demonstrated to sufficient accuracy with the possible exception of the scattering theory and surface chemistry modules. The main challenge now is to develop these modules to the point where their capabilities match those of the probes.

Other challenges include the enhancement of signal-to-noise ratios, especially during operation in actual reactors where samples are rotated for uniformity and may experience mechanical vibration as well. Another issue is the runout of the optical beam that occurs if the surface of the sample is not perpendicular to the rotation axis. Some progress has already been made. Maracas et al. [44] have developed a piezoelectric-based manipulator for MBE where runout can be reduced to acceptable levels by applying appropriate voltages to the transducers. The NCSU group has developed a mechanical equivalent for OMCVD. Woollam and co-workers have demonstrated the capability of maintaining compositions x of $In_{0.53}Ga_{0.47}As$ constant to within 0.1% in an operating multiwafer OMCVD reactor, where the challenges to be met included not only having to average measurements over a number of wafers but also to deal with the dead time that occurs as a result of the gaps between wafers [45]. Even though the composition is not strictly controlled in real time, this accomplishment is still nontrivial.

Finally, techniques for probing the surface reaction layer, which is the closest region to the product and feeds bulk growth, are not yet fully developed and/or tested. Accessing and understanding the properties of this region will be one of the outstanding challenges of the next few years.

ACKNOWLEDGMENTS

It is a pleasure to acknowledge the support of the Defense Advanced Research Projects Agency and the Office of Naval Research under Contracts N-00014-95-1-0962 and N-00014-93-1-0255, respectively.

REFERENCES

1. E. H. A. Granneman, Thin Solid Films **228**, 1 (1993).

2. C. E. Zah, R. Bhat, F. J. Favire, Jr., S. G. Menocal, N. C. Andreadakis, K.-W. Cheung, D.-M. Hwang, M. A. Koza, and T.-P. Lee, IEEE J. Quantum Electronics **27**, 1440 (1991).

3. C. R. Abernathy, J. Vac. Sci. Technol. **A11**, 869 (1993).

4. S. M. Bedair, J. Vac. Sci. Technol. **B12**, 179 (1994).

5. A. C. Jones, J. Cryst. Growth **129**, 728 (1993).

6. M. G. Peters, B. J. Thibeault, D. B. Young, J. W. Scott, F. H. Peters, A. C. Gossard, and L. A. Coldren, Appl. Phys. Lett. **63**, 3411 (1993).

7. B. T. Sullivan and J. A. Dobrowolski, Appl. Opt. **32**, 2351 (1993).

8. S. A. Chalmers and K. P. Killeen, Appl. Phys. Lett. **62**, 1182 (1993).

9. K. P. Killeen and W. G. Breiland, J. Electron. Mater. **23**, 179 (1994).

10. R. M. Lum, M. L. McDonald, J. C. Bean, J. Vandenberg, T. L. Pernell, A. Robertson, and A. Karp, Appl. Phys. Lett. **69**, 928 (1996).

11. D. E. Aspnes, E. Colas, A. A. Studna, R. Bhat, M. A. Koza, and V. G. Keramidas, Phys. Rev. Lett. **61**, 2782 (1988).

12 I. Kamiya, D. E. Aspnes, H. Tanaka, L. T. Florez, J. P. Harbison, and R. Bhat, Phys. Rev. Lett. **68**, 627 (1992).

13. I. Kamiya, D. E. Aspnes, L. T. Florez, and J. P. Harbison, Phys. Rev. **46**, 15894 (1992).

14. D. W. Kisker, P. H. Fuoss, K. L. Tokuda, G. Renaud, S. Brennan, and J. L. Kahn, "X-ray analysis of GaAs surface reconstructions in H_2 and N_2 atmospheres," Appl. Phys. Lett. **56**, 2025 (1990).

15. F. J. Lamelas, P. H. Fuoss, P. Imperatori, D. W. Kisker, G. B. Stephenson, and S. Brennen, Appl. Phys. Lett. **60**, 2610 (1992).

16. W. Richter, Philos. Trans. R. Soc. London **A344**, 453 (1993).

17. C. Pickering, in **Handbook of Crystal Growth**, vol. 3, ed. D. T. J. Hurle (Elsevier, Amsterdam, 1994), 817.

18. J. F. McGilp, Progress in Surface Science **49**, 1, (1995).

19. D. E. Aspnes and I. Kamiya, SPIE Proc. **2730**, 306 (1996).

20. D. E. Aspnes, Thin Solid Films **89**, 249 (1982).

21. D. E. Aspnes, J. P. Harbison, A. A. Studna, and L. T. Florez, J. Vac. Sci. Technol. **A6**, 1327 (1988).

22. S. E. Acosta-Ortiz and A. Lastras-Martinez, Phys. Rev. **B40**, 1426 (1989).

23. N. Kobayashi and Y. Horikoshi, J. Appl. Phys. Jpn. **29**, L702 (1990).

24. N. Kobayashi and Y. Kobayashi, Thin Solid Films **225**, 32 (1993).

25. N. Dietz and H. J. Lewerenz, Appl. Surf. Sci. **69**, 350 (1993).

26. K. J. Bachmann, U. Rossow and N. Dietz, Mater. Sci. & Eng. **B35**, 472 (1995).

27. N. Dietz and K. J. Bachmann, Vacuum **47**, 133 (1996).

28. J. I. Dadap, B. Doris, Q. Deng, M. C. Downer, J. K. Lowell, and A. C. Diebold, Applied Physics Letters 64, 2139-2141 (1994).

29. A. J. Pidduck, D. J. Robbins, A. G. Cullis, D. B. Gasson, and J. L. Glasper, J. Electrochem. Soc. **136**, 3083 (1989).

30. F. G. Celii, E. A. Beam III, L. A. Files-Sesler, H.-Y. Liu, and Y. C. Kao, Appl. Phys. Lett. **62**, 2705 (1993).

31. J. E. Epler and H. P. Schweizer, Appl. Phys. Lett. **63**, 1228 (1993).

32. U. Rossow, L. Mantese, and D. E. Aspnes, Proc. 23rd Internat. Conf. Phys. Semicond. Berlin, M. Scheffler and R. Zimmerman, eds. (World Press, Singapore, 1996), p. 831.

33. C. M. J. Wijers and G. P. M. Poppe, Phys. Rev. **B46**, 7605 (1992).

34. B. S. Mendoza and W. L. Mochán, Phys. Rev. **B53**, R10473 (1996).

35. See, for example, R. M. A. Azzam and N. M. Bashara, **Ellipsometry and Polarized Light** (North-Holland, Amsterdam, 1977).

36. D. E. Aspnes, W. E. Quinn, M. C. Tamargo, M. A. A. Pudensi, S. A. Schwarz, M. J. S. P. Brasil, R. E. Nahory, and S. Gregory, Appl. Phys. Lett. **60**, 1244 (1992).

37. F. H. Pollak and H. Shen, J. Electron. Mater. **19**, 399 (1990).

38. O. J. Glembocki, J. A. Tuchman, K. K. Ko, S. W. Pang, A. Giordana, and C. E. Stutz, Mat. Res. Soc. Symp. Proc. **324**, 153 (1994).

39. D. E. Aspnes, J. Opt. Soc. Am. **10**, 974-83 (1993).

40. P. Chiaradia, G. Chiarotti, S. Nannarone, and P. Sassaroli, Solid State Commun. **26**, 813 (1978).

41. K. Hingerl, D. E. Aspnes, and I. Kamiya, Surface Sci. **287/288**, 686 (1993).

42. K. Uwai and N. Kobayashi, Appl. Phys. Lett. **65**, 150 (1994).

43. M. Zorn, J. Jönsson, A. Krost, W. Richter, J.-T. Zettler, K. Ploska, and F. Reinhardt, J. Cryst. Growth **145**, 53 (1994).

44. G. N. Maracas, C. H. Kuo, S. Anand, R. Droopad, G. R. L. Sohie, and T. Levola, J. Vac. Sci. Technol. **A13**, 727 (1995).

45. C. Herzinger, B. Johs, P. Chow, D. Reich, G. Carpenter, D. Croswell, and J. Van Hove, Mat. Res. Soc. Symp. Proc. **406**, 347 (1996).